Non-Stationary Responses of Cables with Slowly Varying Length*

Stefan Kaczmarczyk† and

School of Mechanical Engineering, University of Natal, Durban 4041, Republic of South Africa

Wieslaw Ostachowicz

Institute of Fluid Flow Machinery, Polish Academy of Sciences, 14 Fiszera Street, 80-952 Gdansk, Poland

(Received 5 January 2000; accepted 12 April 2000)

In this paper the longitudinal dynamics of hoisting cables with time-varying length is investigated. The overall response of a hoisting cable system to inertial load due to transport motion acceleration/deceleration and to external harmonic excitation is studied. A mathematical model of the system is formulated, and the response is simulated numerically. Due to the time-varying length of the cable, the natural frequencies of the system vary slowly, and a transient resonance occurs when one of the frequencies coincides with the frequency of the excitation at some critical time. Near the resonance region the resonant mode is dominant and a single-mode approximation of the system response in this region is formulated. A combined perturbation and numerical technique is applied to predict the response during passage through the main resonance. A numerical study is presented in which the dynamic responses of cables in a deep mine hoisting installation are examined.

* This article is an extended version of a paper presented by the first author at the Sixth International Congress on Sound and Vibration, Copenhagen, July 1999.

† Member of the International Institute of Acoustics and Vibration (IIAV)

1. INTRODUCTION

Structural elements such as ropes and cables are among the oldest tools used by humanity in its quest for technological advancement. For example, a copper wire rope was found in the ruins of Nemeveh near Babylon which originate from about 700 B.C.,[1] and in Pompeii bronze ropes estimated to be 2400 years old have been excavated.[2] These elements are known to have the ability to withstand relatively large axial loads in comparison to bending and torsional loads, and have played an indispensable role in towing operations, in supporting structures, in conducting signals and in systems designed to carry payloads in vertical and inclined transport installations. In this latter application cables are of time-varying length. However, the rate of change is small and the length may be assumed to vary slowly. Consequently, the dynamic characteristics of the system vary slowly during its operation, rendering the system non-stationary.

The responses of systems with non-stationary parameters and excitations are qualitatively different from the responses of stationary systems, especially in the neighbourhood of some critical values of the parameters, when transitions through resonance regions occur. The non-stationary resonance phenomena are often delayed, and frequently accompanied by beat phenomena. Hence, specialised treatment is required in order to analyse the responses of these systems. A number of studies have been carried out in this area. Kevorkian[3] has considered the passage through resonance in a harmonically excited single-degree-of-freedom system with a slowly varying natural frequency. In this study the solution was constructed by matching two asymptotic expansions: the outer expansion away from resonance, and the inner expansion near resonance. Agrawal and Evan-Iwanowski,[4] and Evan-Iwanowski[5] have extended the asymptotic method developed by Mitropolskii[6] for determining resonant responses of non-stationary, non-linear multi-degree-of-freedom systems. The theory and methodology to describe the behaviour of a system evolving slowly through internal resonance has been presented by Ablowitz, Funk and Newell,[7] and also by Kevorkian.[8]

More recently Kevorkian,[9] Bosley and Kevorkian[10] and Bosley[11] have proposed that in order to generate an approximate solution, the slowly varying oscillatory second-order system of N equations can be transformed into a Hamiltonian standard form of $2N$ first-order differential equations using action and angle variables together with the concept of adiabatic invariance. Later perturbation techniques, namely the method of averaging or the method of multiple scales, can be applied to determine the solution.

Alternatively, the perturbation techniques can be applied directly to the second-order model so that a first-order system can be obtained to compute the slowly varying amplitudes and phases for the first approximation of the response. Nayfeh and Asfar,[12] and Neal and Nayfeh[13] used this methodology to study single-degree-of-freedom systems with non-stationary parametric excitations. This technique was also implemented by Tran and Evan-Iwanowski[14] to study the response of the Van der Pol oscillator with non-stationary external excitation, and by Cveticanin[15] in the analysis of non-stationary oscillations of a textile machine rotor.

In this study the longitudinal response to an external excitation of a deep mine hoisting cable with slowly varying length and carrying concentrated inertial elements is investigated. The winding cycle in this hoisting installation consists of three main phases: the acceleration phase, the constant ve-

locity phase, and the deceleration phase. The overall response due to the cycle acceleration/deceleration load and a boundary periodic excitation is determined by direct numerical integration of the discretised model. A single-mode approximation is then used to describe the response near to the primary resonance region, and the method of multiple scales is applied to predict and to analyse the response during the passage through the resonance.

2. EQUATIONS OF MOTION

A typical mine hoist system comprises a driving winding drum, a steel wire cable, a sheave mounted in headgear and a conveyance. The cable passes from the drum over the sheave, forming a horizontal or inclined catenary, to the conveyance constrained to move in a vertical shaft, and forms the vertical rope of time-varying length. A cable storage mechanism on the winder drum is applied in order to facilitate a uniform coiling pattern. A simplified longitudinal model of this arrangement is shown in Fig. 1. In this model the section $l = O_1O$ represents a slowly varying length of this part of the cable that is already coiled onto the winder drum, and the catenary section $OC = L_c$ is represented by a massless spring of constant k_c. Furthermore, the sheave inertial effects are typified by its effective mass M_S, and the end mass M represents the conveyance. The position of an arbitrary section of the cable in the dynamically undeformed (reference) configuration, when the cable total length is given as L_0, is determined by the Lagrangian co-ordinate s measured from O_1. Also, it is assumed that the cable has a constant effective cross-sectional area A, a constant mass per unit length m, and effective Young's modulus E.

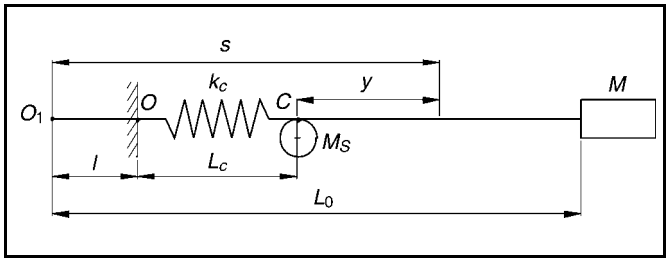

Figure 1. Longitudinal model of a hoisting cable.

The equations governing the dynamic response of the system can be derived by applying the variational approach of analytical mechanics. In this approach Hamilton's principle can be used which yields

$$\int_{t_1}^{t_2}(\delta E - \delta\Pi_e - \delta\Pi_g + \delta W_{nc})\,dt = 0, \tag{1}$$

where E, Π_e, Π_g denote the system kinetic energy, the cable elastic strain energy, and the system gravitational potential energy, respectively, and δW_{nc} represents the virtual work of the damping forces. Consequently, the longitudinal dynamic displacement u of the rope is described by the partial differential equation[16]

$$\rho u_{,tt} - \mu_1 EAu_{,sst} + \mu_2 \rho u_{,t} - EAu_{,ss} =$$

$$f(s,t) + \left[k_c u_l(t) - M_S u_{,st}\dot{l}\right]\delta(s - L_1), \tag{2}$$

with the boundary conditions given as

$$k_c u(L_1^-, t) - EAu_{,s}(L_1^-, t) = 0, \tag{3}$$

$$EAu_{,s}(L_0^+, t) = 0, \tag{4}$$

where $(\,)_{,s}$ denotes partial differentiation with respect to s, $(\,)_{,t}$ designates partial differentiation with respect to time, and the overdot indicates total differentiation with respect to time. The mass distribution function of the system is given as $\rho = m + M_S\delta(s - L_1) + M\delta(s - L_0)$, where $L_1 = l + L_c$. Also, $s = L_1^-$ denotes the point immediately to the left of C, $s = L_0^+$ indicates the point immediately to the right of M, and δ is the Dirac delta function. The system is subjected to boundary excitation at $s = l$, represented by a prescribed periodic function $u_l(t)$, and to the inertial load due to an overall transport motion, given by $f(s,t) = \rho\ddot{l}$. It should be noted also, that the term $M_S u_{,st}\dot{l}$ appears in the equation of motion. This component represents the sheave inertial effects, and can be deduced from the sheave kinetic energy, given as $E_s = \frac{1}{2}M_S\dot{q}_S^2$, where $\dot{q}_S = u_{,t}(L_1, t) - \dot{l}$. Consequently, Hamilton's procedure leads to the derivative $\frac{d}{dt}\left(\frac{\partial E_s}{\partial \dot{q}_S}\right)$, so that the sheave inertial load is introduced into Eq. (2).

Damping in the system is represented by a viscous proportional damping model, with the internal and external damping effects accommodated in the coefficients μ_1 and μ_2, respectively. Moreover, upon assuming that the modulus E of the cable material is high, the strain of the cable wound around the drum can be neglected, and the length of the cable coiled onto the winder drum is then given as $l(t) = l(0) \pm \int_0^t V(\xi)d\xi$, where V is a prescribed winding velocity, and signs "+" and"−" correspond to ascending and descending respectively, and $l(0)$ is the initial length.

3. APPROXIMATE SOLUTION

3.1. Overall Response

In order to determine the longitudinal response during the entire winding cycle an approximate solution to the equations of motion can be sought using the Rayleigh-Ritz method. Thus, the motion is assumed in the form of the series

$$u = \sum_{n=1}^{N_{long}} Y_n(s,l)z_n(t), \tag{5}$$

where $z_n(t)$ are generalised co-ordinates, and Y_n are free-oscillation modes of the system with the parameter l considered to be instantaneously frozen. These modes are given by the following equation

$$Y_n(s,l) = \cos\gamma_n y(s,l) + \left(\frac{1}{L_c\gamma_n} - \gamma_n\frac{M_S}{m}\right)\sin\gamma_n y(s,l), \tag{6}$$

where $\gamma_n = \omega_n(l)/c$, with $c = \sqrt{EA/m}$, and ω_n represents the longitudinal natural frequency, and $y = s - L_1$. The eigenvalues γ_n are determined from the frequency equation

$$\left(\frac{1}{L_c} - \frac{M_S}{m}\gamma_n^2\right)\left(\cos\gamma_n L_v - \frac{M}{m}\gamma_n\sin\gamma_n L_v\right) -$$

$$\gamma_n\left(\frac{M}{m}\gamma_n\cos\gamma_n L_v + \sin\gamma_n L_v\right) = 0, \tag{7}$$

where $L_v = L_0 - L_1$.

Substituting the expansion Eq. (5) into Eq. (2), multiplying the result by Y_r, by integrating from L_1^- to L_0^+, accounting for the boundary conditions Eqs. (3)-(4), and using the orthogonality properties of the eigenfunctions Y_n, yields a set of equations of the form

$$\ddot{z}_r + \mu_2 \dot{z}_r + \omega_r^2 z_r =$$

$$-\frac{1}{m_r}\sum_{n=1}^{N_{long}}\left[2\dot{l}C_{rn} - EA\Lambda_{rn} + M_S\dot{l}\left(\frac{1}{L_c} - \frac{M_S}{m}\gamma_n^2\right)\right]\dot{z}_n -$$

$$\frac{1}{m_r}\sum_{n=1}^{N_{long}}\left(\dot{l}^2 D_{rn} + \ddot{l}C_{rn} - EA\dot{l}B_{rn} + \mu_2\dot{l}C_{rn} + M_S\dot{l}^2\Gamma_n\right) z_n +$$

$$g_r(t) + Z_r(t),\ r = 1, 2, \ldots, N_{long}, \tag{8}$$

where

$$\begin{aligned}
m_r &= \int_{L_1^-}^{L_0^+}\rho(s)Y_r^2 ds,\\
B_{rn} &= \int_{L_1^-}^{L_0^+}\mu_1 Y_r\frac{\partial Y_{n,ss}}{\partial l}ds,\\
C_{rn} &= \int_{L_1^-}^{L_0^+}\rho(s)Y_r\frac{\partial Y_n}{\partial l}ds,\\
D_{rn} &= \int_{L_1^-}^{L_0^+}\rho(s)Y_r\frac{\partial^2 Y_n}{\partial l^2}ds,\\
\Gamma_n &= \gamma_n(\gamma_n - 2\frac{M_s}{m}\frac{d\gamma_n}{dl}),\\
\Lambda_{rn} &= \int_{L_1^-}^{L_0^+}\mu_1 Y_r Y_{n,ss}ds,\\
g_r(t) &= \frac{1}{m_r}k_c u_l(t),\\
Z_r &= \frac{1}{m_r}\int_{L_1^-}^{L_0^+} f(s,t)Y_r ds.
\end{aligned} \tag{9}$$

Furthermore, in this formulation the boundary excitation is given as $u_l(t) = u_0\cos\Omega t$, where the amplitude u_0 is defined by the geometry of the cable storage mechanism on the winder drum, and the frequency $\Omega = n\omega_d$, where n is an integer and ω_d denotes the drum frequency.

The model represented by Eq. (8) forms a system of second order ordinary differential equations with time-varying coefficients. These coefficients depend on the eigenvalues γ_n that must be determined from the transcendental frequency equation given by Eq. (7). In general, it is not feasible to obtain an exact closed-form solution to time-varying coupled systems of ordinary differential equations. In the problem under consideration, the most convenient approach to solving the system is by direct numerical integration.

3.2. Response at the Resonance Region

When a single term is taken in the expansion Eq. (5) the result is referred to as a single-mode approximation, and the system is reduced to a single-degree-of-freedom model. This simple model has been used extensively and successfully in the analysis of free and forced vibrations of structures.[17] The dynamic behaviour of the cable system near the resonance region is of particular interest. Since the resonant mode is dominant in the system response during the passage through the primary resonance, the single-mode approximation given as

$$u = Y_r(s, l)z_r(t), \tag{10}$$

where Y_r denotes the resonant mode shape function, can be applied to investigate the response at the resonance. Substituting this form into Eq. (2) and applying the Rayleigh-Ritz procedure yields

$$\ddot{z}_r + \omega_r^2(l)z_r =$$

$$-\frac{1}{m_r(l)}\left[2\dot{l}C_{rr}(l) - EA\Lambda_{rr}(l) + M_S\dot{l}\left(\frac{1}{L_c} - \frac{M_S}{m}\gamma_r^2(l)\right) + m_r(l)\mu_2\right]\dot{z}_r -$$

$$\frac{1}{m_r(l)}\left(\dot{l}^2 D_{rr}(l) + \ddot{l}C_{rr}(l) - EA\dot{l}B_{rr}(l) + \mu_2\dot{l}C_{rr}(l) + M_S\dot{l}^2\Gamma_r(l)\right)z_r +$$

$$K_r(l)\cos\Omega t + Z_r(t), \tag{11}$$

where $K_r = k_c u_0/m_r$.

The natural frequency and coefficients in Eq. (11) are expressed in terms of the slowly varying length parameter l, and can be determined using Eq. (9). Two time scales are defined in order to seek an approximate solution to the problem. The first one, a fast non-dimensional scale, is determined as $T = \omega_0 t$, where $\omega_0 = \omega_r(l(0))$. The second scale is a slow scale defined as $\tau = \varepsilon T$, and a variation of l is observed on this scale. During the ascending constant velocity winding phase this length is given as $l = l(0) + V_c t$, where V_c denotes the nominal winding velocity. Assuming $l(0) = 0$, and defining the small parameter as $\varepsilon = V_c/(\omega_0 L_{v0})$, where $L_{v0} = L_v(l(0))$, yields $l = L_{v0}\tau$. Assuming that damping is small, so that one may set $\mu_1 = \varepsilon\mu_1^*$, and $\mu_2 = \varepsilon\mu_2^*$, the following equation, valid for the constant velocity phase, is obtained

$$\frac{d^2 z_r}{dT^2} + \tilde{\omega}_r^2(\tau)z_r = \varepsilon f_r(\tau, \frac{dz_r}{dT}) + \tilde{K}_r(\tau)\cos\tilde{\Omega}T + O(\varepsilon^2), \tag{12}$$

where $\tilde{\omega}_r = \omega_r/\omega_0$, $\tilde{\Omega} = \Omega/\omega_0$, $\tilde{K}_r = K_r/\omega_0^2$, and

$$f_r(\tau, \frac{dz_r}{dT}) = \frac{1}{m_r(\tau)}\left[EA\frac{L_{v0}}{V_c}\Lambda_{rr}(\tau) - 2l' C_{rr}(\tau) - M_S l'\left(\frac{1}{L_c} - \frac{M_S}{m}\gamma_r^2(\tau)\right)\right]\frac{dz_r}{dT} - \frac{L_{v0}}{V_c}\mu_2\frac{dz_r}{dT}. \tag{13}$$

The method of multiple scales is applied to seek an approximate solution to Eq. (12). Thus, the solution is assumed to be of the form[18]

$$z_r = z_{r0}(\phi_r, \tau) + \varepsilon z_{r1}(\phi_r, \tau) + O(\varepsilon^2), \tag{14}$$

where ϕ_r represents a new fast scale, defined as $\phi_r = \int_0^T \tilde{\omega}_r(\varepsilon\xi)d\xi$. Since near the resonance values $\tilde{\omega}_r(\tau)$ are near $\tilde{\Omega}$, a slowly varying detuning parameter $\sigma_r(\tau)$ is introduced to quantify this nearness, so that one can write $\tilde{\Omega} - \tilde{\omega}_r(\tau) = \varepsilon\sigma_r(\tau)$. Setting $\tilde{K}_r = 2\varepsilon\tilde{k}_r$, and implementing the procedure of multiple scales results, in the first approximation, in the solution given as

$$z_r = a_r\cos(\tilde{\Omega}T - \psi_r) + O(\varepsilon), \tag{15}$$

where the amplitude a_r and phase ψ_r are determined by a system of first order differential equations with slowly varying coefficients of the form

$$a_r' = -\frac{1}{2}\left\{\frac{\tilde{\omega}_r'}{\tilde{\omega}_r} - \frac{1}{m_r(\tau)}\left[EA\frac{L_{v0}}{V_c}\Lambda_{rr}(\tau) - 2l'C_{rr}(\tau) - M_S l'\left(\frac{1}{L_c} - \frac{M_S}{m}\gamma_r^2(\tau)\right)\right] - \frac{L_{v0}}{V_c}\mu_2\right\}a_r + \frac{k_r}{\tilde{\omega}_r}\sin\psi_r;$$

$$\psi_r' = \sigma_r(\tau) + \frac{k_r}{\tilde{\omega}_r a_r}\cos\psi_r, \qquad (16)$$

where the prime denotes the derivative with respect to τ. Eqs. (16) do not easily lend themselves to an analytical solution. However, both a_r and ψ_r are slowly varying functions, and the system Eqs. (16) can be solved numerically without difficulty using standard integration methods.

4. NUMERICAL EXAMPLE AND DISCUSSION

4.1. The Deep Mine Winder and Rope Parameters

The parameters of the double drum rock winder at Elandsrand Gold Mine are used to carry out numerical calculations. These parameters are shown in Table 1, and represent a typical deep mine hoisting system operating in South Africa. The Elandsrand Mine winder drum is equipped with a $180^0 - 180^0$ Lebus arrangement to achieve a repetitive coiling pattern during a winding cycle. In this mechanism, the winder drum surface is covered by parallel circular grooves with two diametrically opposed cross-over zones per drum circumference. Each zone offsets the grooves by half a cable diameter and when the cable passes through a cross-over an additional axial displacement relative to the nominal transport motion occurs. The magnitude of this displacement can be calculated as approximately equal to the difference between the arc length transversed through the cross-over and the corresponding diametrical arc. This gives the amplitude $u_0 = \sqrt{(R_d\beta)^2 + d^2/4} - R_d\beta$, where R_d is the drum radius, d represents the cable diameter, and β is the angle defining the diametrical arc corresponding to the cross-over region.[16] As the cross-over occurs twice per drum revolution the frequency of the excitation is equal to twice that of the drum frequency, that is $\Omega = 2V_c/R_d$.

Table 1. Elandsrand simulation parameters.

Total winding cycle time [s]	163
Acceleration/deceleration time [s]	26
Nominal hoisting velocity V_c [m/s]	16
Total hoisted mass M [kg]	23,649
Sheave wheel moment of inertia I [kgm^2]	25,690
Winder drum radus R_d [m]	2.77
Sheave wheel radius R [m]	2.77
Coil cross-over arc β [rad]	0.1
Cable diameter d [m]	48×10^{-3}
Cable linear density m [kg/m]	9.75
Cable effective steel area A [m^2]	1.053×10^{-3}
Cable effective Young's Modulus E [N/m^2]	1.25×10^{11}
Catenary length L_c [m]	73
Maximum depth of winding $L_{v\max}$ [m]	2,204

The longitudinal damping coefficient μ_1 is assumed to be a function of the vertical rope mean tension given as $T_v^i(s) = [M + m(L_0 - s)]g$, where g, denotes the acceleration of gravity, and $L_1 \le s \le L_0$. Namely, μ_1 decreases with increasing mean tension. This is consistent with the results of the experimental investigations,[19-21] and it can be argued that when the tension is increased, the wire strands are more readily locked, and the inter-strand relative motion is constrained, resulting in the coefficient μ_1 being decreased. Following the experimental data reported by Goroshko and Savin,[20] this coefficient is determined as $\mu_1 = (0.5 + \frac{23000}{3500 + 0.75\times10^{-5}\,T_v^i/A}) \times 10^{-4} s$. The value of the second longitudinal damping coefficient is assumed to be $\mu_2 = 0.159 s^{-1}$, as established by tests performed by Constancon.[22] Also, the effective sheave mass is determined as $M_S = I/R^2$.

4.2. Overall Dynamic Response

The total longitudinal dynamic behaviour of the system is described by the set of linear ordinary differential Eqs. (8), and the solution of these equations, combined with the expansion Eq. (5), gives the overall longitudinal response. The coefficients in Eqs. (8) are slowly time-varying, and the system is referred to as a linear time-varying system.[23] In general, it is not feasible to obtain an exact closed-form solution to time-varying coupled systems of ordinary differential equations. Approximate analytical studies to predict the response of such systems could be carried out by perturbation methods.[4] However, the algebra in these techniques is quite involved. An alternative method was presented by Shahruz and Tan,[24] who found an approximate closed-form solution to the response of linear slowly varying systems under external

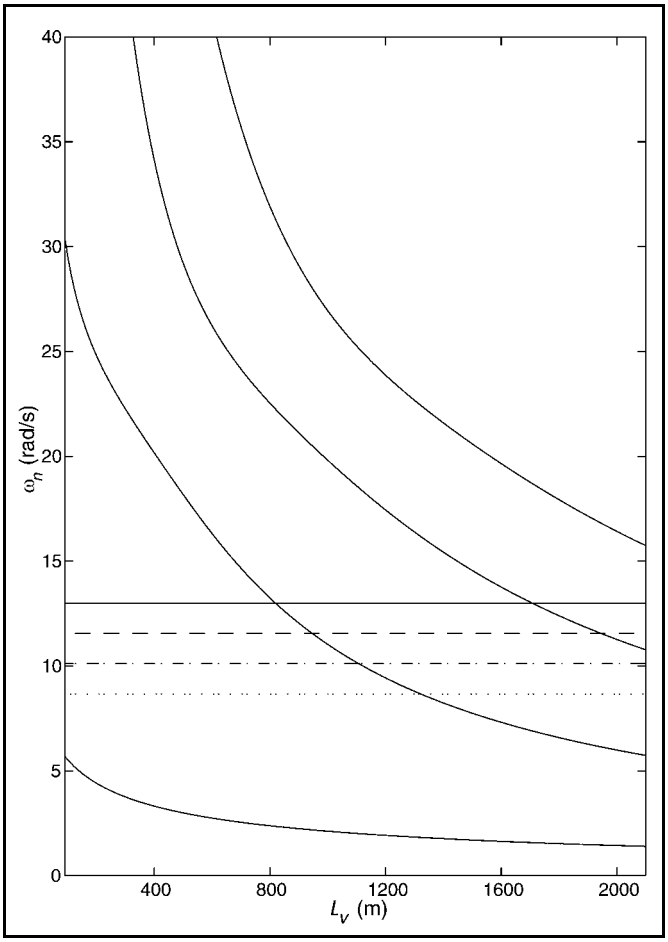

Figure 2. Longitudinal frequency curves for the Elandsrand Mine winder, with horizontal lines denoting the frequency of excitation Ω, corresponding to various nominal winding velocities $V_c = 12$ (⋯), 14 (−·−), 16 (−−), and 18 (—) m/s.

excitations using the technique of freezing slowly varying parameters. This technique, however, is not suitable for the general case when the eigenvalues of the frozen system cannot be obtained explicitly in terms of the frozen time parameter. Thus, the most convenient approach to solving the system of Eqs. (8) is by direct numerical integration.

Since the highest dynamic forces in hoisting cables occur during the up-wind, the simulation is carried out for the ascending cycle, when a fully loaded conveyance is being raised from the bottom of the shaft. The natural frequencies of the system vary slowly during the entire wind due to the slowly varying length of the vertical rope. This is illustrated in Fig. 2, where the first four up-wind longitudinal natural frequencies, determined from the transcendental Eq. (7), are plotted against the vertical cable length. Frequencies of the excitation Ω, corresponding to various winding velocities V_c, are also shown in this diagram. As one can observe, the natural frequencies increase with the shortening length of the vertical rope. It can be noted that for the nominal winding velocity of 16 m/s, a transition through resonance occurs twice: at the beginning of the cycle when the excitation frequency coincides with the third natural frequency at approximately $L_v = 1950\,\text{m}$, and later during the wind when a passage through the second natural frequency takes place at approximately $L_v = 950\,\text{m}$.

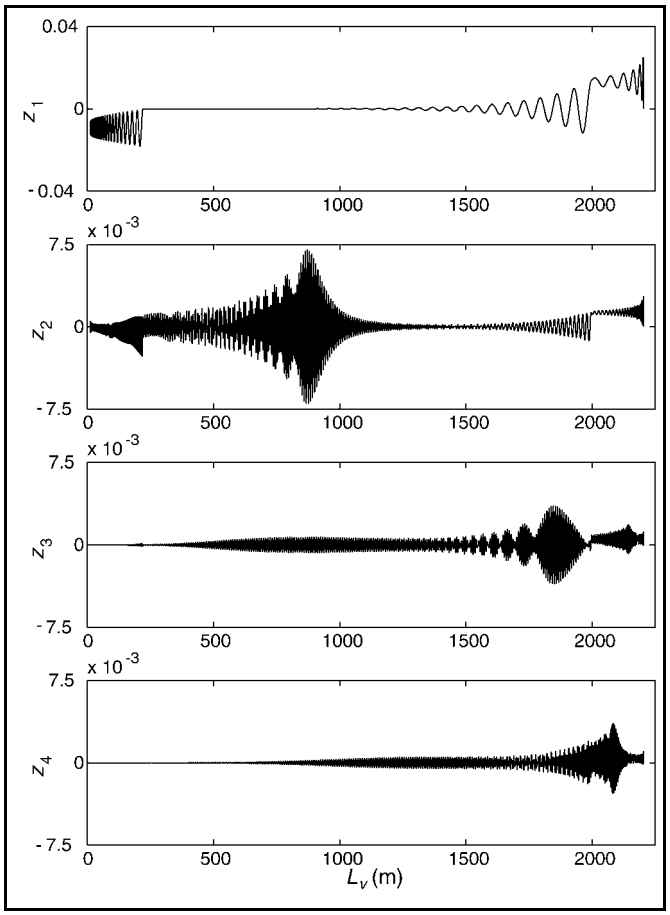

Figure 3. Longitudinal modal co-ordinates for the Elandsrand Mine winder simulation at the nominal winding velocity $V_c = 16$ m/s.

It is evident that the system eigenvalues are widely spread, especially at the end of the wind, and therefore the complete solution to the problem will consist of slow and fast components. Thus, the dynamics of the deep mine winder system represents a *stiff* problem,[25] and if the numerical solution is to return the entire transient response of the system over a long time interval, integration must be performed using a relatively large time step to cover the slow components. However, the time step must be also small enough to capture the fast components, and to keep the numerical solution within acceptable bounds. Thus, due to these requirements integration methods not designed for stiff problems are ineffective, and lead to unstable results when applied to stiff equations.

The problem of numerical integration of systems of stiff ordinary differential equations has attracted considerable attention, and a number of efficient integration algorithms that allow relatively large time steps, and that guarantee stability and bounded numerical error are available.[26,27] Multistep methods based on backward differentiation formulas (BDF's, also known as Gear's method), have been the most prominent and most widely used for solving stiff problems. Recently, a new family of formulas called the numerical differentiation formulas (NDF's) have been developed and implemented in the MATLAB ODE suite.[28] They are more efficient than the BDF's, though the higher order formulas in this family are somewhat less stable. Both BDF's and NDF's codes are available from the ode15s MATLAB solver.

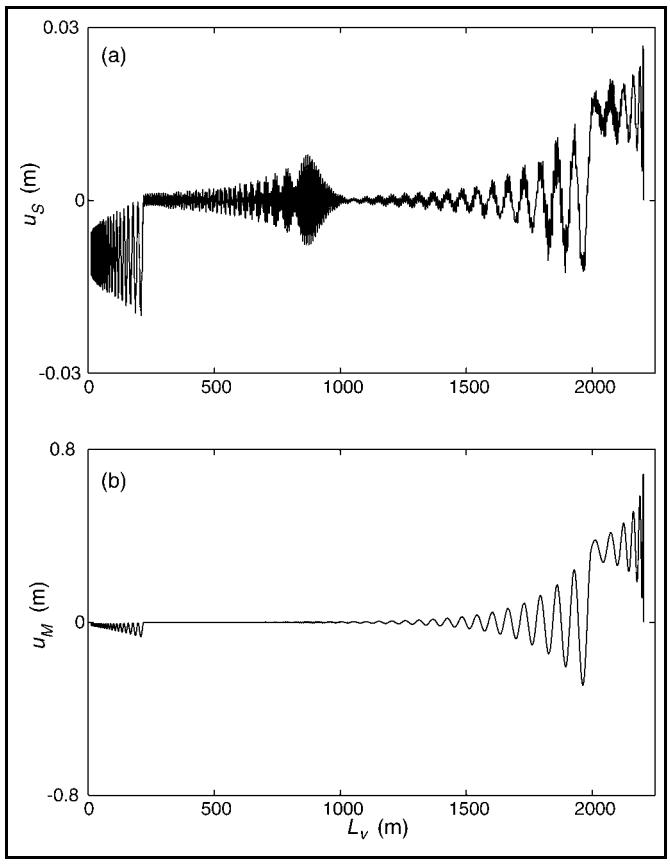

Figure 4. Longitudinal response of the Elandsrand cable system at the nominal winding velocity $V_c = 16$ m/s: (a) at the sheave; (b) at the conveyance.

The non-stationary modal Eqs. (8), with the number of modes $N_{long} = 4$, have been integrated numerically in the MATLAB 5 computing environment using the ode15s solver, with the default numerical differentiation formulas, and with the default *relative accuracy tolerance* and *absolute error tolerances* of 10^{-3} and of 10^{-6}, respectively. The simulation results for the nominal winding cycle are shown in

Figs. 3-6. The generalised modal co-ordinates z_n, $n = 1, \ldots, 4$, are plotted against the vertical rope length L_v in Fig. 3. The displacements at the sheave and at the conveyance, given as

$$u_S = \sum_{n=1}^{4} Y_n(L_1, l) z_n(t), \tag{17}$$

$$u_M = \sum_{n=1}^{4} Y_n(L_0, l) z_n(t), \tag{18}$$

respectively, are shown in Fig. 4. The plots of the total catenary tension T_c, and of the total vertical rope tension T_S at the sheave and T_M at the conveyance, together with the tension ratio across the sheave, versus L_v are presented in Fig. 5.

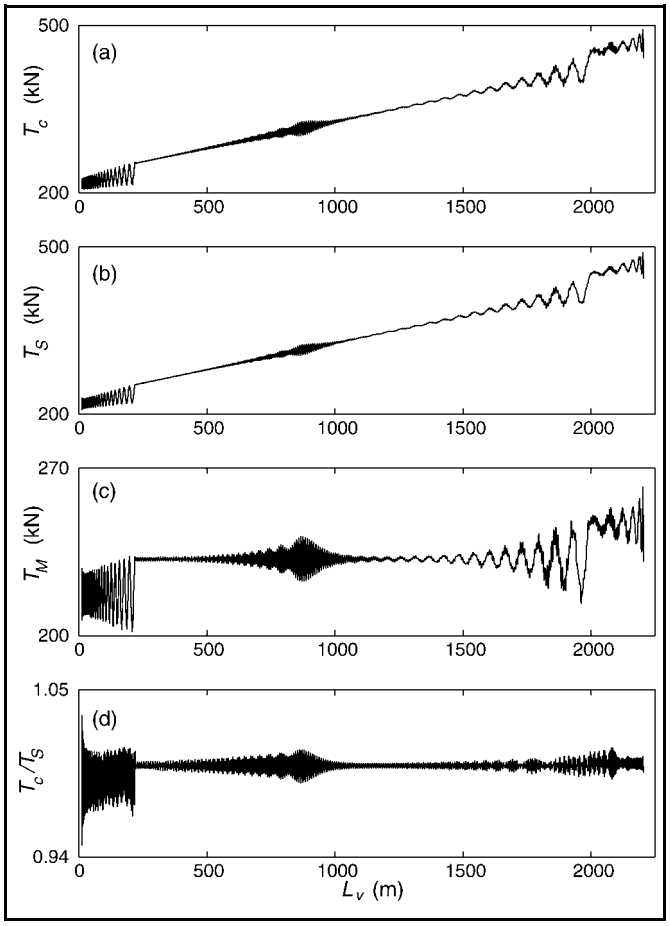

Figure 5. Total cable tensions for the Elandsrand Mine winder at the nominal velocity $V_c = 16$ m/s: (a) the catenary tension T_c; (b) the vertical rope tension T_S at the sheave; (c) the vertical rope tensionT_M at the conveyance; (d) the tension ratio across the sheave T_c/T_S.

In these plots the tensions are determined as follows. The total catenary tension is calculated as

$$T_c(t) = T_c^i(t) + T_{cd}(t), \tag{19}$$

where the slowly varying mean catenary tension is represented by $T_c^i = T_v^i(L_1)$, and the catenary dynamic tension is defined as

$$T_{cd} = k_c \left[\sum_{n=1}^{4} z_n(t) - u_I(t) \right]. \tag{20}$$

Subsequently, the total vertical rope tension is defined as

$$T_v(s,t) = T_v^i(s) + T_{vd}(s,t), \tag{21}$$

where the dynamic component T_{vd} is expressed using the Kelvin-Voigt viscoelastic model, whereby the normal stress is related to the strain and strain rate, namely

$$T_{vd}(s,t) = EA[u_{v,s} + \mu_1(s) u_{v,ts}]. \tag{22}$$

Hence, the rope tensions at the sheave and at the conveyance are given as $T_S = T_v(L_1, t)$, and $T_M = T_v(L_0, t)$, respectively. The vertical rope dynamic tensions are given as $T_{Sd} = T_{vd}(L_1, t)$ at the sheave and $T_{Md} = T_{vd}(L_0, t)$ at the conveyance. Subsequently, the catenary and vertical rope dynamic tensions are plotted against L_v in Fig. 6.

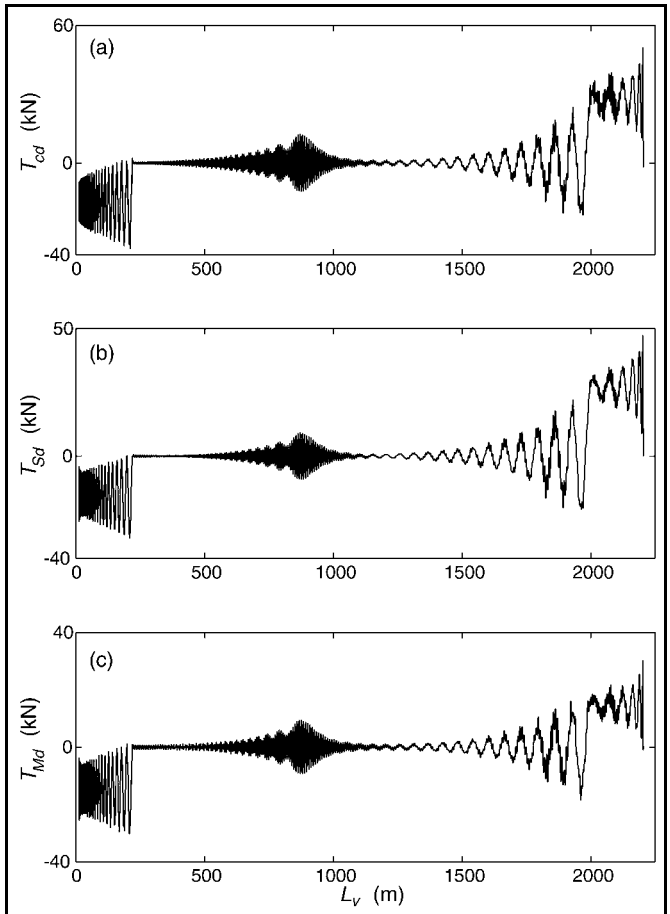

Figure 6. Dynamic cable tensions for the Elandsrand Mine winder at the nominal velocity $V_c = 16$ m/s: (a) the catenary dynamic tension T_{cd}; (b) the vertical rope dynamic tension T_{Sd} at the sheave; (c) the vertical rope dynamic tension T_{Md} at the conveyance.

The results demonstrate various transient vibration phenomena that occur during the wind. A significant response due to the initial acceleration/final deceleration inertial loads at the beginning, and at the end of the cycle, respectively, is predicted. This response is prominent both at the sheave and at the conveyance. Referring to the modal co-ordinate plots, it is evident that the fundamental mode dominates in the resulting transient oscillations, as recorded in the co-ordinate z_1 plot. As anticipated earlier from the frequency diagram, passages through resonance are manifested in the response plots. The co-ordinate z_2 displays resonance behaviour in the

region $\Omega = \omega_2$, and the co-ordinate z_3 demonstrates transition through the resonance condition $\Omega = \omega_3$. These resonance phenomena affect especially the sheave response, which can be seen in Fig. 4.

The total cable tensions reflect the system dynamics during the wind. The dynamic components oscillate about the corresponding mean values, that for the catenary and at the sheave increase with the vertical length. The tension ratio across the sheave is close to unity over the entire cycle, demonstrating a small increase at the end of the wind, but remaining in the limits of approximately $0.94 - 1.05$. The influence of acceleration/deceleration, and of transitions through resonance on the cable tensile forces is better illustrated in Fig. 6. It can be seen, that significant oscillations in the dynamic tensions are predicted during the initial and final stages of winding due to the acceleration/deceleration inertial loads. Also, at a depth of approximately $700 - 1000$ m, the resonance condition $\Omega = \omega_2$ produces substantial tension oscillations. The effect of this main resonance on the system dynamics is discussed in more detail in the following.

4.3. Response at the Resonance Region

The single-mode response of the system near the resonance is given by Eqs. (10) and (15), with the slowly varying amplitude and the phase determined by the system of first order differential Eqs. (16). These autonomous ordinary differential equations with variable coefficients do not easily lend themselves to an analytical solution. Analytical methods for analysis of problems of this type are very few and tend to be either difficult to apply or limited in application to a small class of systems. For example, Raman, Bajaj and Davies[29] treated analytically classical non-linear vibratory systems in the presence of non-stationary excitation. They discussed passage through primary resonance in the forced Duffing's oscillator, described by the averaged first order equations for the amplitude and phase. An analytical study of the response was presented using matched asymptotic expansions. This technique is however applicable only within a small neighbourhood of the instability region, and various beating phenomena associated with the passage cannot be predicted by this approach. As shown by Nayfeh and Mook,[18] direct numerical integration of non-stationary amplitude-phase equations is perhaps the most convenient approach. The amplitude a_r and phase ψ_r governed by Eqs. (16) are slowly varying functions, and the system can be solved numerically without difficulty using standard integration methods. In this study the MATLAB ode23 solver based on an explicit Runge-Kutta (Eqs. (2) and (3)) pair of Bogacki and Shampine[27] has been used to determine the solution in this study.

The accuracy of this solution and of the first approximation given by Eq. (15) can be verified by comparison with the overall response obtained earlier from the system of Eq. (8). This comparison is shown in Fig. 7, where the passage through the resonance region $\Omega = \omega_2$ (that is for $r = 2$) in the Elandsrand system operating at the nominal hoisting velocity $V_c = 16$ m/s is illustrated. In Fig. 7(a) the response envelope, determined as $a_S = Y_2(L_1, l)a_2$, is superimposed on the sheave response obtained from Eq. (17). The rope dynamic tensions T_{Sd} at the sheave and T_{Md} at the conveyance, calculated using the expansion Eq. (5) and Eq. (22), with superimposed tension envelopes are shown in Fig. 7(b) and Fig. 7(c), respectively. The tension envelopes are determined from Eq. (22) using the single-mode representation Eq. (10) together with the approximation Eq. (15), and are given by

$$E_{vd}(s,\tau) = EA\sqrt{A_r^2 + B_r^2}\,, \tag{23}$$

where

$$A_r(s,\tau) = \left(\frac{\partial Y_r}{\partial s} + \mu_1 \frac{\partial^2 Y_r}{\partial s \partial l} V_c\right) a_r + \mu_1 \varepsilon \omega_0 \frac{\partial Y_r}{\partial s} a_r'; \tag{24}$$

$$B_r(s,\tau) = \mu_1(\varepsilon\omega_0 \psi_r' - \Omega)\frac{\partial Y_r}{\partial s} a_r. \tag{25}$$

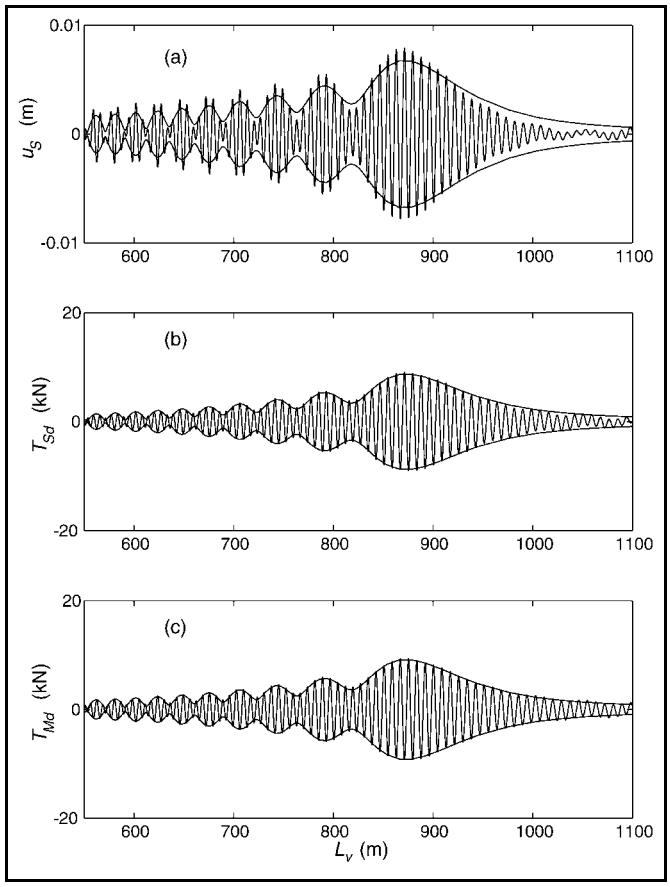

Figure 7. Overall response and dynamic cable tensions for the Elandsrand Mine winder at the nominal velocity $V_c = 16$ m/s with superimposed envelope curves obtained from the multiple scales model at the resonance region: (a) the sheave response; (b) the rope tension at the sheave; (c) the rope tension at the conveyance.

It can be seen that in the resonance region the single-mode solution approximates well the overall response and tension curves.

Transition through the resonance region $\Omega = \omega_2$ is further illustrated in Fig. 8. In Fig. 8(a) the non-stationary frequency-response curves are shown, with the amplitudes a_2 plotted against the detuning parameter σ_2, and in Fig. 8(b) these amplitudes are shown against the vertical length (depth) L_v, for four winding velocities, namely $V_c = 12, 14, 16,$ and 18 m/s. It should be noted, that these amplitudes represent directly the maximum sheave motions, as the resonant modes Y_r in Eq. (10) are normalised to the unity at the sheave end. It can be seen that the resonance region is reached at higher depths for lower values of the winding velocities, while the detuning parameter σ_2 decreases when making a single passage through zero. This is consistent with the frequency dia-

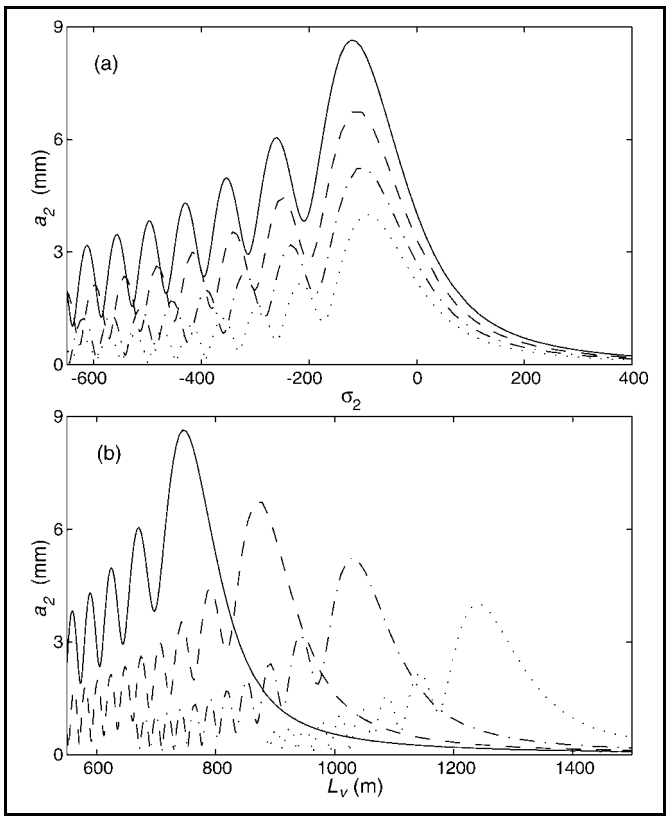

Figure 8. Non-stationary amplitude response during passage through resonance in the Elandsrand Mine system: (a) the frequency-response curves; (b) amplitudes against the vertical length, for the winding velocities $V_c = 12$ (⋯), 14 (– · –), 16 (– –), and 18 (—) m/s.

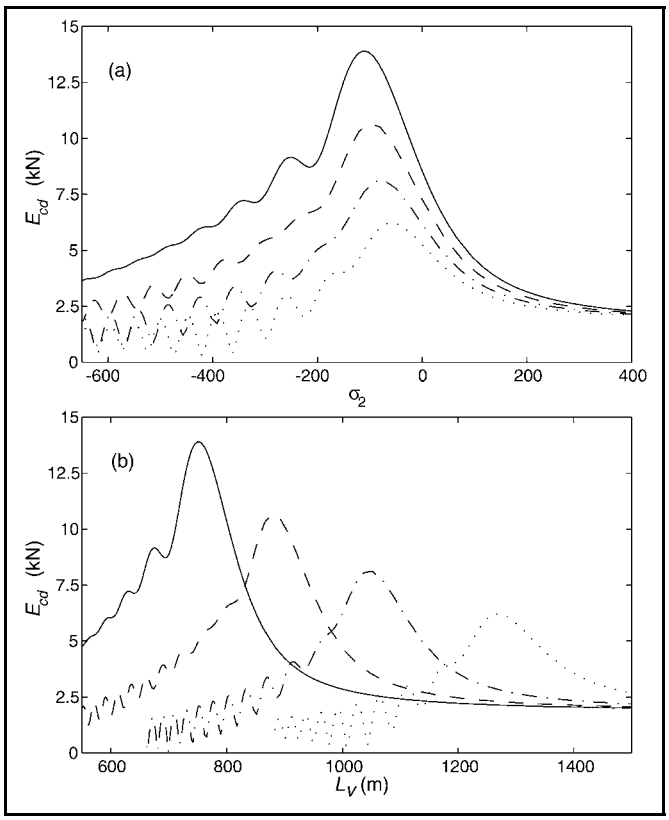

Figure 10. Catenary dynamic tension envelopes during passage through resonance in the Elandsrand Mine system shown (a) against the frequency detuning parameter; (b) against the vertical length, for the winding velocities $V_c = 12$ (⋯), 14 (– · –), 16 (– –), and 18 (—) m/s.

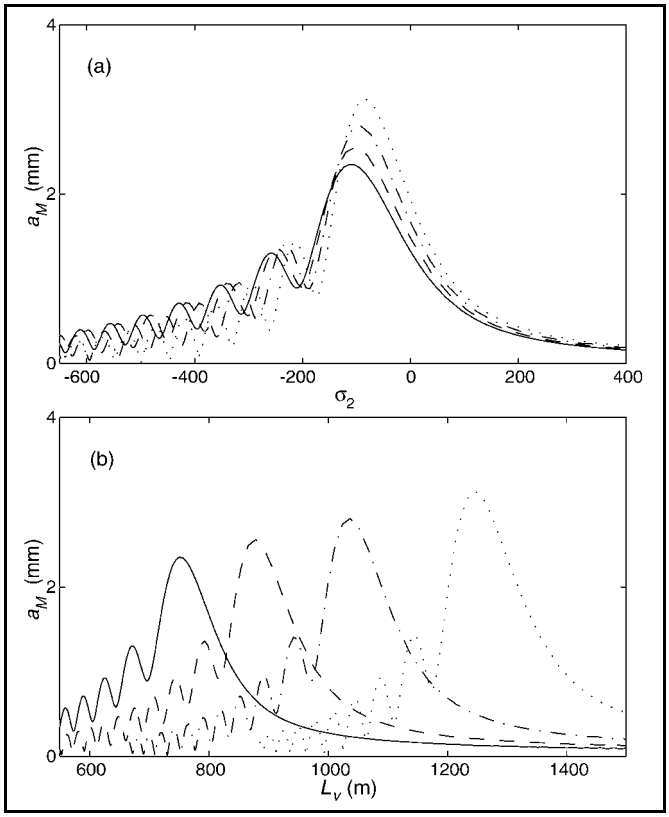

Figure 9. Conveyance amplitude response during passage through resonance in the Elandsrand Mine system: (a) the non-stationary frequency-response curves; (b) amplitudes against the vertical length, for the winding velocities $V_c = 12$ (⋯), 14 (– · –), 16 (– –), and 18 (—) m/s.

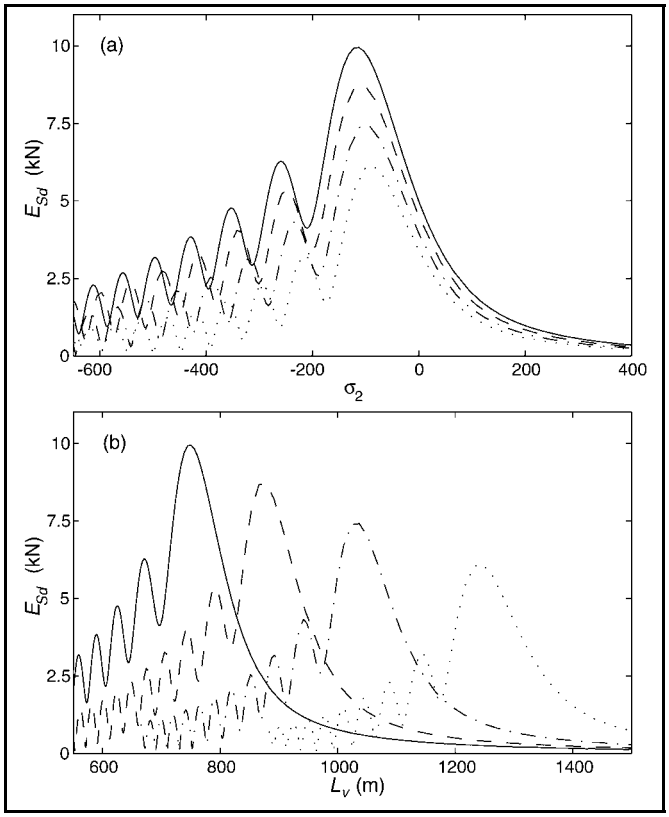

Figure 11. Sheave dynamic tension envelopes during passage through resonance in the Elandsrand Mine system shown (a) against the frequency detuning parameter; (b) against the vertical length, for the winding velocities $V_c = 12$ (⋯), 14 (– · –), 16 (– –), and 18 (—) m/s.

gram shown in Fig. 2, where the resonance regions for the corresponding velocities can be identified against the depth. The amplitudes start growing when the resonance region is approached, and near the resonance ($\sigma_r \approx 0$) they increase rapidly, and decline afterwards due to damping, developing damped beat phenomena. The period of the beats decreases with time. It can be observed that the higher the winding velocity, the higher the maximum value of the corresponding amplitude. A different pattern of behaviour can be identified at the conveyance end, which is illustrated in Figs. 9(a) and 9(b), where the conveyance amplitude envelope curves, determined as $a_M = Y_r(L_0, l)a_2$, are represented against the frequency detuning parameter and against the depth, respectively. As one can see, in this case higher maximum values of amplitudes are recorded for lower winding velocities.

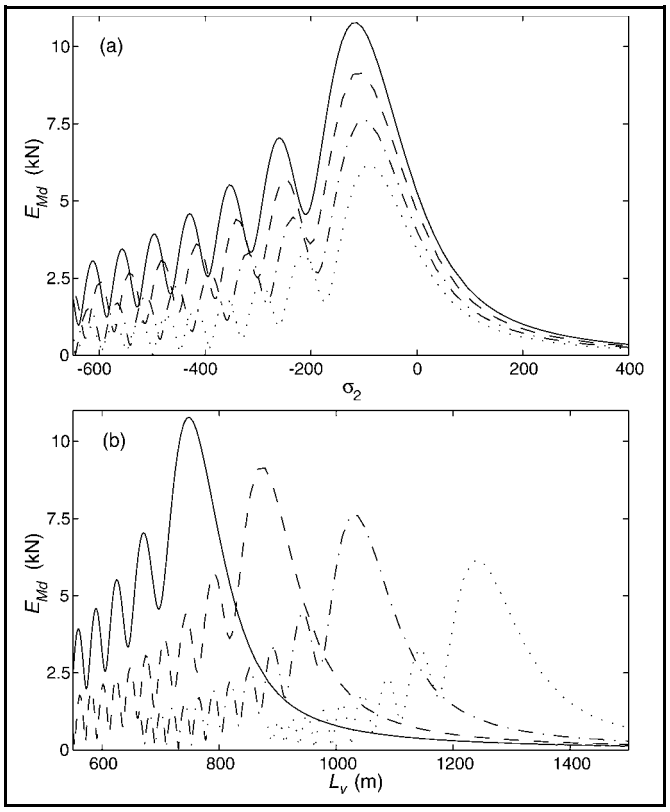

Figure 12. Conveyance dynamic tension envelopes during passage through resonance in the Elandsrand Mine system shown (a) against the frequency detuning parameter; (b) against the vertical length, for the winding velocities V_c = 12 (⋯), 14 (– · –), 16 (– –), and 18 (—) m/s.

The upper envelopes of the dynamic tensions, namely E_{cd} of the catenary cable, E_{Sd} of the rope at the sheave and E_{Md} at the conveyance, are plotted against the detuning parameter and the vertical length in Figs. 10, 11 and 12, respectively. The catenary tension envelopes are determined using Eq. (20) where the single-mode solution Eq. (15) is applied, so that

$$E_{cd} = k_c \sqrt{(a_r \cos \psi_r - u_0)^2 + (a_r \sin \psi_r)} \,. \qquad (26)$$

The rope tension envelopes are found from Eq. (23). It is evident from the tension envelope plots that the tension amplitudes increase rapidly during the passage through resonance, declining slowly afterwards. Both in the catenary and in the vertical rope the tension amplitudes demonstrate the tendency to reach higher values for higher velocities.

5. SUMMARY AND CONCLUSIONS

The overall longitudinal dynamic behaviour of a deep mine hoisting cable system is demonstrated in the numerical simulation of the double drum winder system at the Elandsrand Gold Mine. The simulation results illustrate a transient response due to the acceleration/deceleration inertial load and passages through primary longitudinal resonances, when the frequency of the excitation due to a coiling mechanism at the winding drum coincides with the natural frequencies during the motion cycle. Also, significant dynamic fluctuations in the cable tensions are predicted. The tension ratio across the sheave is close to the unity which indicates that frictional slip will not occur.

The effect of transitions through the primary resonances is investigated using a combined perturbation and numerical technique. A single-mode model is applied to represent the system during a passage through resonance. It accommodates the fundamental feature of the system, namely its non-stationary nature, and adequately represents the main type of vibration occurring in the system. The multiple scales method is used which leads to a system of first order ordinary differential equations for the amplitude and phase of the response. These are slowly varying functions and the system can be solved numerically without difficulty. The accuracy of this solution is verified against the overall response obtained from a numerical simulation of the original second order ordinary differential equations of motion. It is shown that the single-mode model approximates well the system in the main resonance region.

The analysis demonstrates that the main resonance is reached at higher depths for lower values of hoisting velocities. The amplitude plots reveal that the more rapid the passage through resonance, the smaller the maxima of the conveyance response, and the higher the maxima of the response at the sheave. The amplitudes decline after the passage due to damping developing beat phenomena. The dynamic cable tensions also grow rapidly during the passage, and reach higher levels for higher hoisting velocities.

The proposed model and the computational algorithm form an efficient method to assess and to analyse the dynamic behaviour of deep mine hoisting cables.

6. ACKNOWLEDGEMENT

The support received from the University of Natal Research Fund is gratefully acknowledged.

REFERENCES

[1] Costello, G.A. *Theory of Wire Rope*, Springer-Verlag, New York, (1990).

[2] Glushko, M.F. *Steel Hoisting Cables*, Technika, Kiev, (1966) (in Russian).

[3] Kevorkian, J. Passage Through Resonance For a One-Dimensional Oscillator with Slowly Varying Frequency, *SIAM Journal of Applied Mathematics*, **20** (3), 364-373, (1971).

[4] Agrawal, B.N., and Evan-Iwanowski, R.M. Resonances in Non-stationary, Nonlinear, Multidegree-of-Freedom Systems, *AIAA Journal*, **11** (7), 907-912, (1973).

[5] Evan-Iwanowski, R.M. *Resonance Oscillations in Mechanical Systems*, Elsevier Scientific Publishing Company, Amsterdam, (1976).

[6] Mitropolskii, Y.A. *Problems of the Asymptotic Theory of Nonstationary Vibrations*, Israel Program for Scientific Translations Ltd., Jerusalem, (1965).

[7] Ablowitz, M.J., Funk, B.A., and Newell, A.C. Semi-Resonant Interactions and Frequency Dividers, *Studies in Applied Mathematics*, **L11** (1), 51-74, (1973).

[8] Kevorkian, J. Resonance in a Weakly Nonlinear System with Slowly Varying Parameters, *Studies in Applied Mathematics*, **62**, 23-67, (1980).

[9] Kevorkian, J. Perturbation Techniques for Oscillatory Systems with Slowly Varying Coefficients, *SIAM Review*, **29**, 391-461, (1987).

[10] Bosley, D.L., and Kevorkian, J. Sustained Resonance in Very Slowly Varying Oscillatory Hamiltonian Systems, *SIAM Journal of Applied Mathematics*, **51** (2), 439-471, (1991).

[11] Bosley, D.L. An Improved Matching Procedure for Transient Resonance Layers in Weakly Nonlinear Oscillatory systems, *SIAM Journal of Applied Mathematics*, **56** (2), 420-445, (1996).

[12] Nayfeh, A.H., and Asfar, K.R. Non-Stationary Parametric Oscillations, *Journal of Sound and Vibration*, **124** (3), 529-537, (1988).

[13] Neal, H.L., and Nayfeh, A.H. Response of a Single-Degree-of-Freedom System to a Non-Stationary Principal Parametric Excitation, *International Journal of Non-Linear Mechanics*, **25** (2/3), 275-284, (1990).

[14] Tran, M.H., and Evan-Iwanowski, R.M. Non-Stationary Responses of Self-Excited Driven systems, *International Journal of Non-Linear Mechanics*, **25** (2/3), 285-297, (1990).

[15] Cveticanin, L. The Oscillations of a Textile Machine Rotor on Which the Textile is Wound up, *International Journal of Mechanism and Machine Theory*, **26** (3), 253-260, (1991).

[16] Kaczmarczyk, S. The Passage Through Resonance in a Catenary-Vertical Cable Hoisting System with Slowly Varying Length, *Journal of Sound and Vibration*, **208** (2), 243-269, (1997).

[17] Szemplinska-Stupnicka, W. *The Behavior of Nonlinear Vibrating Systems*, Kluver Academic Publishers, Dordrecht, (1990).

[18] Nayfeh, A.H., and Mook, D.T. *Nonlinear Oscillations*, John Wiley & Sons, New York, (1979).

[19] Vanderveldt, H.H., and Gilheany, J.J. Propagation of a Longitudinal Pulse in Wire Ropes under Axial Loads, *Experimental Mechanics*, **10**, 401-407, (1970).

[20] Goroshko, O.A., and Savin, G.N. *Introduction to Mechanics of One-Dimensional Bodies with Variable Length*, Naukova Dumka, Kiev, (1971) (in Russian).

[21] Mankowski, R.R., and Cox, F.J. Response of Mine Hoisting Cables to Longitudinal Shock Loads, *Journal of the South African Institute of Mining and Metallurgy*, **86**, 51-60, (1986).

[22] Constancon, C.P. The Dynamics of Mine Hoist Catenaries, PhD Thesis, Faculty of Engineering, University of the Witwatersrand, Johannesburg, (1993).

[23] D'Angelo, A. *Linear Time-Varying Systems: Analysis and Synthesis*, Allyn and Bacon, Inc., Boston, (1970).

[24] Shahruz, S.M., and Tan, C.A. Response of Linear Slowly Varying Systems Under External Excitations, *Journal of Sound and Vibration*, **131** (2), 239-247, (1989).

[25] Nikravesh, P.E. *Computer-Aided Analysis of Mechanical Systems*, Prentice-Hall Inc., Englewood Cliffs, (1988).

[26] Hairer, E., and Wanner, G. *Solving Ordinary Differential Equations II. Stiff and Differential - Algebraic Problems*, Springer-Verlag, Berlin Heidelberg, (1991).

[27] Shampine, L.F. *Numerical Solution of Ordinary Differential Equations*, Chapman & Hall, New York, (1994).

[28] Shampine, L.F., and Reichelt, M.W. MATLAB Version 5 Help Documentation, The Matlab ODE suite, (1996).

[29] Raman, A., Bajaj, A.K., and Davies, P. On the Slow Transition Across Instabilities in Nonlinear Dissipative Systems, *Journal of Sound and Vibration*, **192** (4), 835-865, (1996).